Environmental Engineering and Management Journal

March 2019, Vol.18, No. 3, 727-735
http://www.eemj.icpm.tuiasi.ro/; http://www.eemj.eu

"Gheorghe Asachi" Technical University of Iasi, Romania

REMOVAL OF NH^+_4-N FROM AQUEOUS SOLUTION BY CERAMSITE COATED WITH $Mg(OH)_2$ COMBINED WITH AIR STRIPPING

Tianpeng Li[1,2], Tingting Sun[2], Dengxin Li[1*]

[1]College of Environment Science and Engineering, Donghua University, Shanghai 201620, PR China
[2]College of City and Architecture Engineering, Zaozhuang University, Zaozhuang, Shandong 277160, PR China

Abstract

Removal of excessive ammonium nitrogen (NH^+_4-N) from aqueous solution has been of considerable concern for several decades. It can be removed by air stripping, a necessary prerequisite is adding enough alkali. This study presented the first attempt to investigate the potential use of ceramsite coated with magnesium hydroxide (CCMH) on the effectiveness of NH^+_4-N removal coupled with air stripping at ambient temperature without alkali addition. The results showed that the CCMH coupled with air stripping process has the highest NH^+_4-N removal efficiency, after stripping for 150 min, the removal rates were 86.4%, 90.7% and 93.8% at pH 3, 7 and 11, respectively. This demonstrated that in acidic condition, the combined process still had high removal efficiency. It was further determined that the changes of initial pH had no significant effect on the NH^+_4-N removal. As air flow rate increased, the removal rate of NH^+_4-N naturally increased. Besides, the removal rates of NH^+_4-N followed the general first-order model in the investigated initial pH and air flow rates, with the general first-order rate constants rapidly increased. In conclusion, the combined process can be considered as a promising method for the removal of NH_4^+-N from aqueous solution, having high removal efficiency, pH value adjustment free and the stripped ammonia can be absorbed without secondary pollution.

Keywords: air stripping, ammonium nitrogen, ceramsite, magnesium hydroxide

Received: July, 2016; Revised final: October, 2016; Accepted: October, 2016; Published in final edited form: March, 2019

1. Introduction

Nitrogen compounds, are not only nutrients essential to all forms of life, but also are largely used as an indispensable chemical in various industries from manufacturing fertilizers to animal feed. In aqueous environments, they mainly occur in the form of NH^+_4-N (Song et al., 2018). But, NH^+_4-N present in receiving waters at excess levels is undesirable, causes depletion in dissolved oxygen (DO), because it is easily oxidized by bacteria and converted into nitrite and nitrate; causes eutrophication, acts as a nutrient for algae and other microorganisms; and toxic to sensitive aquatic biota. Moreover, environmental regulations regarding NH^+_4-N in industrial and agricultural wastewaters that flows to nitrogen-sensitive receiving waters are becoming steadily more stringent in many developing and developed countries. For example, in China, the 12th Five-Year Plan articulates a challenging task of a 10% discharge reduction in total NH^+_4-N from 2010 to 2015 (Yuan et al., 2016). The discharge standards of NH^+_4-N have also been established for municipal wastewater treatment plants in China and were set to 5 and 8 mg N/L for A and B standard of first grade effluent, respectively, and 25 mg N/L for second grade effluent. Therefore, to eliminate the adverse environment effect of NH^+_4-N, the concentrations of NH^+_4-N were to be reduced to below the inhibitory level, no matter what origin, is not a trivial (Reli et al., 2015).

Presently, several methods have been developed and applied for the removal of NH^+_4-N from aqueous solution. Biological process of nitrification and denitrification is known as the most

*Author to whom all correspondence should be addressed: e-mail: lidengxin@dhu.edu.cn; Phone: +86 2167792541; Fax: +862167792522

economic and efficient method for removal of NH^+_4-N from sewage (Wang et al., 2015). However, the removal of NH^+_4-N by biological method is transformed to dinitrogen gas (N_2) and therefore cannot be recovered and reused (Malovanyy et al., 2013). Chemical precipitation of NH^+_4-N removal by adding magnesium salt and phosphate to form magnesium ammonium phosphate hexahydrate (MAP) is considered as an effective method (Yetilmezsoy and Sapci-Zengin, 2009). Obviously, the method requires the addition of chemical reagents, which may introduce new pollutants. Breakpoint chlorination, as practiced for many years in the water treatment industry, provides an additional physical-chemical means for removing NH^+_4-N from sewage (Pressley et al., 1972). Previous studies have confirmed that the reaction of chlorine with NH^+_4-N may form toxic disinfection by-products (DBPs), which may cause possible public health risks (Zhou et al., 2016). Photocatalytic oxidation (Ding et al, 2018) and adsorption (Arslan and Veli, 2012) have been in use in various types of wastewater treatments for the removal of NH^+_4-N. However, photocatalytic oxidation method using organic resins as carrier are very expensive, and improving the adsorption capacity of adsorbents is the focus of adsorption process.

Air stripping has been reported as an economical and efficient physical method for remove NH^+_4-N from aqueous solution (Gustin and Marinsek-Logar, 2011; Ata et al., 2017), with many outstanding advantages. One is that it is relatively simple and stable. The other is that it is unaffected by toxic compounds, that could disrupt the performance of a biological system (Rubia et al., 2010). In addition, the concentrated gaseous ammonia purged after stripping can be recovered and absorbed by sulfuric acid (H_2SO_4) solution, forming ammonium sulfate ($(NH_4)_2SO_4$) fertilizer for agricultural use. Necessarily, air stripping requires either direct addition of alkaline compounds, such as sodium hydroxide (NaOH), potassium hydroxide (KOH) and calcium hydroxide ($Ca(OH)_2$), to elevate the pH or heat to increase the temperature (generally above 60 ^oC) to release the free ammonia. Unfortunately, the direct introduction of chemical compounds can increase the amount of sludge precipitates, form pipe scale, or cause mechanical problems. Thus, it has become the center of attention of different research groups to choose appropriate hydroxides to create a basic condition for air stripping.

Magnesium hydroxide (MH), an environmental friendly material (Matsukevich et al., 2017), possesses a large specific surface area, high activity, and extraction ability. In laboratory scale, many methods have been developed to synthesize MH, including precipitation, hydrothermal and sol-gel method. MH is usually used in has attracted considerable attention because of its wide range of applications, such as flame retardant composite formulations (Tai et al., 2007), adsorption of anionic dye (Zhang et al., 2014) and antacid to neutralize stomach acid and laxatives (Kaza et al., 2012). However, the fine particle size of MH makes it very difficult to separate from the water phase, which limits its application in wastewater treatment. Coated technology can provide a preferable attempt to solve the above problem. So, selection of an appropriate loading material has become a hotspot of research.

Ceramsite, as filter material (Mittelman et al., 2015), loading material (Li et al., 2017), carrier in a biofilter (Wang et al., 2016) and adsorbent (Li et al., 2018), has been widely applied in wastewater treatment. Due to similar mineral contents, more and more solid wastes (Furlani et al., 2011; Wang and Zhang, 2013), including sewage sludge, river or marine sediment, low quality fly ash, construction and demolition (C&D) and glass cullet, were selected as a potential substitute to replace natural resources for production of ceramiste. To our best knowledge, little study has been reported to use ceramsite coated with MH and then combined with air stripping to treatment of wastewater containing NH^+_4-N so far.

The objective of this study was to assess the removal efficiency of NH^+_4-N from aqueous solution by CCMH coupled with air stripping at ambient temperature without pH adjustment. Firstly, the ceramsite and MH were prepared by high-temperature sintering process and direct precipitation method, respectively, and then CCMH was fabricated by impregnation method. Secondly, the samples were characterized by SEM-EDS, XRD, FTIR and BET. Finally, the optimum removal processes were determined, subsequently, the effect of initial pH and air flow rate on the NH^+_4-N removal efficiency were investigated, and the removal kinetics were analyzed.

2. Experimental

2.1. Materials and chemicals

The sludge, fly ash and river sediment were obtained from Shanghai Songjiang Sewage Treatment Plant, Shanghai Waigaoqiao Power Generation Co. Ltd, Songjiang Campus of Donghua University, China, respectively, and their compositions are listed in Table 1. Ammonium Chloride (NH_4Cl), magnesium chloride ($MgCl_2 \cdot 6H_2O$) and NaOH were purchased from Sinopharm Chemical Reagent Co., Ltd, China. All chemicals appeared in this study were of analytical grade and were used as received without further purification. Deionized water was applied for all the experiments.

Table 1. Chemical composition of raw materials (%)

Raw materials	*SiO_2*	*Al_2O_3*	*Fe_2O_3*	*CaO*	*MgO*	*Na_2O*	*K_2O*	*Ignition loss*
Sludge	7.5	2.3	6.9	2.9	0.5	0.1	0.5	72.4
River sediment	52.5	17.6	5.1	1.5	1.8	0.5	2.8	8.5
Fly ash	56.8	25.7	7.0	8.1	0.8	0.4	1.9	0.2

2.2. Preparation of CCMH

The ceramsite was prepared from sludge, fly ash and river sediment, with a mass ratio of 5:4:1. 10-mm-diameter green bodies were produced manually by adding a necessary amount of deionized water. After dried completely, they were sintered at a temperature of 300ºC for 20 min. The temperature was then increased to 1150ºC for 5 min to ensure combustion and decomposition of the binder and to form micrometer- and nanometer-sized pores in the interior (Ji et al., 2010), followed by natural cooling to room temperature over 120 min. Finally, the ceramsite were crushed down and sieved to be diameters of about 1 mm and were washed with deionized water to remove the water-soluble residues and other undesirable material, and they were stored in a vacuum desiccator for surface coating after dried in an oven at 105ºC for about 4 h.

1000 mL MH emulsion was synthesized by direct precipitation method, using $MgCl_2 \cdot 6H_2O$ and NaOH with a definite Mg^{2+}/OH^{-1} mole ratio of 1: 2. After about 10 min, 50 g ceramsite were added into the emulsion. And the CCMH was produced through employing dipcoating techniques after stirring 60 min at 80ºC. After this, the CCMH was washed several times using deionized water, centrifugation and dried in vacuum at 70ºC over 10 h.

2.3. Batch tests

A volume of 1000 mg/L stock solution was prepared by dissolving 3.819 g of NH_4Cl in 1000 mL deionized water. 50 mL volume simulated wastewater in different concentrations of NH_4^+-N in the range of 400-500 mg/L were prepared by stepwise dilution of the stock solution. The batch tests were carried out at ambient temperature and the procedure was as follows: a 100 mL breaker was placed on a magnetic stirrer (150 rpm) in which 50 mL of simulated wastewater was first poured, the initial pH of solution was adjusted with 0.1 M NaOH or 0.1 M HCl to obtain designed value and then 3.5 g agent was added into this solution. Immediately, air was introduced into the mixture via an air pump (ACO-001, Guangdong Risheng Group Co., Ltd, China), the desired air flow rates (0.4, 0.8 and 1.6 L/min) were controlled by a flow meter.

Air charged with ammonia was bubbled through 1 M H_2SO_4 solution. After a designated time, regulate the effluent pH, in order to eliminate the interference of magnesium ion (Mg^{2+}), and then the NH_4^+-N concentration in the filtrate was measured. All of the experiments were performed twice under the same conditions and an averaged value was employed.

2.4. Analytical methods

The composition of raw materials was measured by X-ray fluorescence spectrometry (XRF, model XRF-1800, Shimadzu Corporation, Japan). The crystalline phases of samples were characterized by X-ray diffraction (XRD, D/max- 2550 PC, Shimadzu Corporation, Japan) with CuK a radiation (λ= 0.1548 nm) at 40 kV and 40 mA. A Scanning Electron Microscope-Energy Dispersive Spectrometer (SEM-EDS, Quanta- 250, Fei Instrument, Czech) was used to observe the surface morphology of samples with an accelerating voltage of 13 kV. The surface of samples was sputtered with gold layer in order to improve the quality of the images.

Fourier Transform Infrared Spectrophotometer (FTIR, Bruker Tensor 27, Germany) was employed to study the chemical structures of samples, FTIR spectra were taken on a KBr disk at a frequency range of 4000-400 cm^{-1}. The specific surface area, S_{BET}, was calculated by applying the Brunauer-Emmett-Teller (BET) equation. The average pore radius was estimated from the relation $2Vp/S_{BET}$, where Vp is the total pore volume (at $P/P_0 = 0.2$). Pore size distribution over the mesopore range was generated by the Barrett-Joyner-Halenda (BJH) analysis of the desorption branches, and the values for the average pore size were calculated. The concentration of NH_4^+-N was detected using Nessler's reagent (HgI_2-KI-NaOH) spectrophotometrically at a wavelength of 420 nm according to the China's industrial standard (HJ 535-2009). The NH_4^+-N removal efficiency is expressed according to the measured results (Eq. 1).

$$R = \frac{C_0 - C_t}{C_0} \times 100\% \quad (1)$$

where: R is the removal rate of NH_4^+-N, %; C_0 and C_t are the concentration of NH_4^+-N at initial and time t min, respectively, mg/L.

3. Results and discussion

3.1. Characterization

The XRD patterns of the samples are given in Fig. 1. As shown in Fig. 1(a), the chemical compositions of the ceramsite included various metal oxides and metal compounds, such as syn-Fe_2O_3, Quartz-SiO_2, Albite, Labradorite and Anorthite. A number of researchers have demonstrated that heavy metals are properly stabilized in ceramsite during sintering process and cannot be easily released into the environment again to cause secondary pollution (Xu et al., 2009; Han et al., 2013). From Fig. 1(b), it was found that compared with ceramsite, some new peaks at 2θ diffraction angle of 19.28, 34.12, 37.68 and 49.06 appeared in the XRD pattern of CCMH. Reference to the XRD pattern database (International Centre for Diffraction Data, ICDD), these new peaks were corresponding to the different crystal planes of MH. Therefore, we can draw a conclusion that CCMH can be obtained under the synthetic conditions.

The SEM images and EDS spectra of the samples are presented in Fig. 2 and it can be seen that

a clear change in their surface morphology was revealed. As Fig. 2(a) indicated that the surface of ceramsite is quite smooth and highly polished, where has coarse, irregular and porous surface, with a large number of well-developed uneven holes and cracks inside. As Fig. 2(b) illustrated that after coated with MH, the surface of ceramsite became rough and appeared a large amount of sediment. According to the results of Fig. 1, it is believed that the sediment is MH. The EDS spectra indicated that before and after coated, the content of Mg element in ceramsite increased from 0.0 to 28.4 (wt%). The results suggested that MH existed on the surface and porous of ceramsite.

As shown in Fig. 3, the FTIR spectra revealed that there were great similarities between ceramsite and CCMH. Both the samples exhibit some strong adsorption peaks at about 3450.57, 1641.38 and 1386.78 cm^{-1}, were assigned to stretching vibration of hydroxyl functional groups including hydrogen bonding due to adsorbed water, out-of-plane rocking vibration of O-C-O, bending vibration of C-O-H and stretching vibration of C=O (Li et al., 2011; He et al., 2015). Compared with the spectrum of ceramsite, a new adsorption peak appeared at about 3701.31 cm^{-1} in the spectrum of CCMH, probably attributed to the bending and stretching vibration of the hydroxyl (-OH) bond in the crystal structure of MH (Feng and Sun, 2015; Zou et al., 2016). Another change was the adsorption peak at about 1122.54 cm^{-1}. The results further implied that the functional group (-OH) was grafted on the surface of ceramsite.

A typical N_2 adsorption-desorption isotherms of the samples are displayed in Fig. 4, from which it was evident that the adsorption-desorption patterns of the samples belong to the typical IUPAC IV-type with the H_2-type hysteresis loop, which is a characteristic of particles with uniform size and mesoporous structure (Basahel et al., 2015). Both the samples showed type IV isotherms with hysteresis loop at P/P_o = 0.45 to 0.95. Whereas, each sample exhibited a different type of hysteresis loop suggested that pore size and shape were not same in these samples. As detailed in Fig. 4(a), the S_{BET}, average pore volume and pore diameter of ceramsite were found to be about 0.73 m^2/g, 0.004 cm^2/g and 18.87 nm, respectively. From Fig. 4(b), it was indicated that the S_{BET}, average pore volume and pore diameter of CCMH were 29.99 m^2/g, 0.141 cm^2/g and 17.75 nm, respectively. Compared with that of the ceramsite, the S_{BET} and average pore volume of CCMH were improved about 41.1 and 35.3 times, respectively.

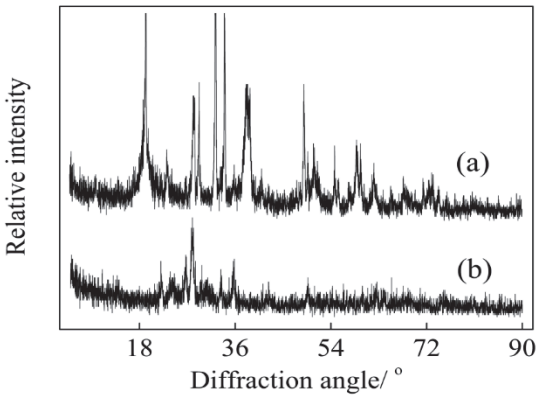

Fig. 1. XRD patterns of (a) CCMH and (b) ceramsite

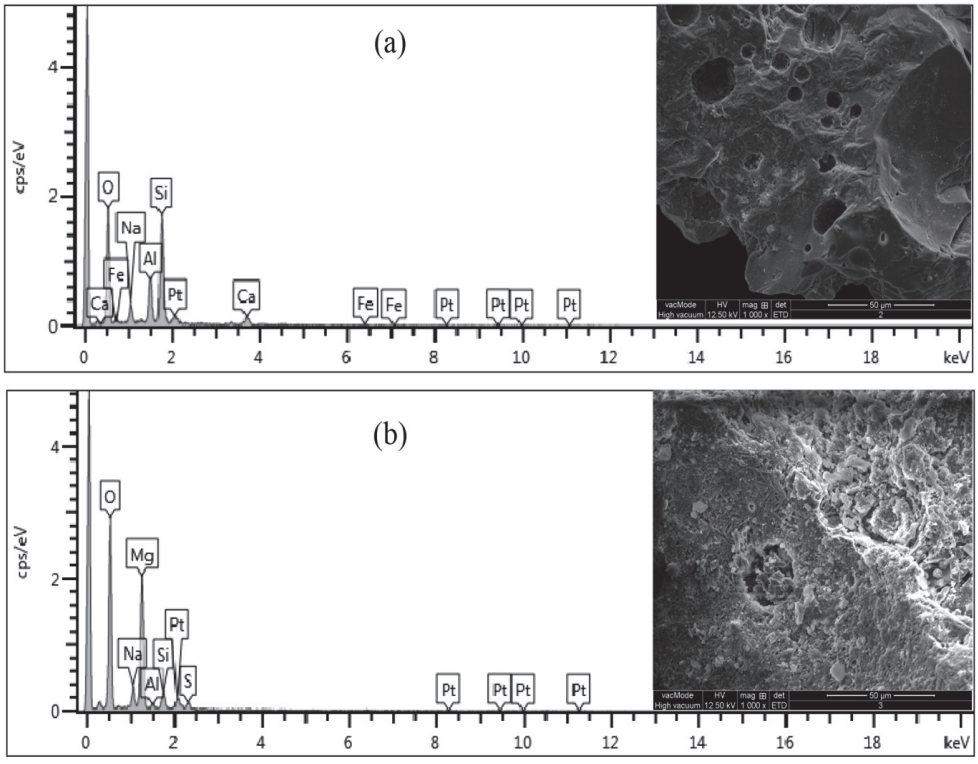

Fig. 2. SEM images and EDS spectra of (a) ceramsite and (b) CCMH

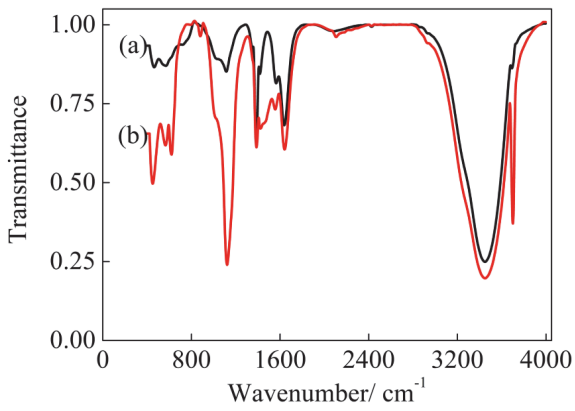

Fig. 3. FTIR spectra of (a) ceramsite and (b) CCMH

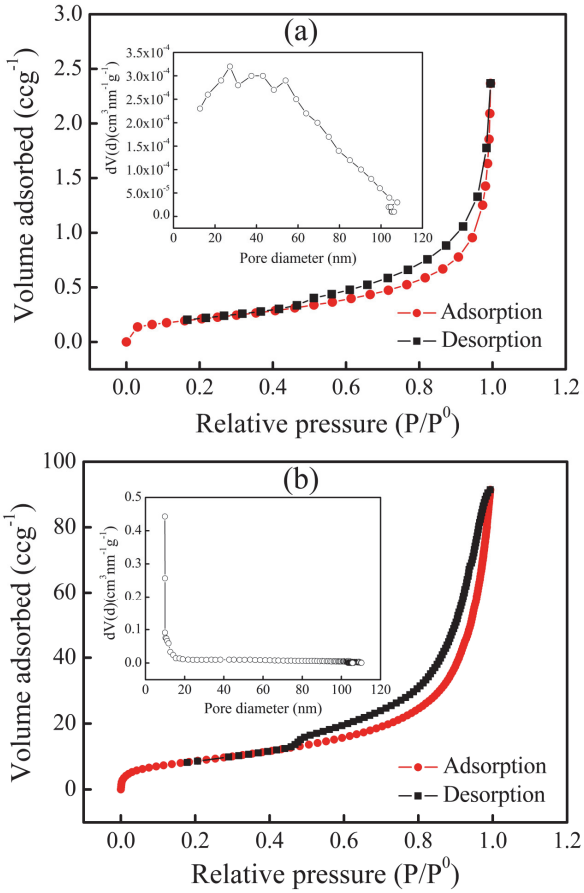

Fig. 4. N_2 adsorption-desorption isotherms and pore size distribution (inset) of (a) ceramsite and (b) CCMH

3.2. Theoretical analysis

In water bodies, the equilibrium relationship between the ammonium ion (NH^+_4) and the aqueous ammonia ($NH_{3(aq)}$) always exists, as follows (Lee, 2003):

$$NH^+_4 + H_2O \Leftrightarrow NH_{3(aq)} + H_3O^+ \quad (2)$$

where the pK_A and ΔH^o of Eq. 2 were 9.25 at 25 °C, and 12.42 Kcal/mol, respectively.

Furthermore, the equilibrium relationship between the $NH_{3(aq)}$ and the gas ammonia ($NH_{3(gas)}$) may also exist, is given by Eq. 3 (Jr et al., 2002).

$$NH_3(aq) \Leftrightarrow NH_3(gas) \quad (3)$$

As Eqs. 2 and 3 illustrated that removal of NH_4^+-N from aqueous solution require two steps. The Step I involves the conversion of NH^+_4 to $NH_{3(gas)}$ (ammonia dissociation equilibrium). The Step II is the diffusion of $NH_{3(gas)}$ to the air-water interface into the air above (involved water-side mass transfer and air-side mass transfer) (Limoli et al., 2016). In order to realize the Step I, the pH value of the system should be raised over 7 or above (Zhang et al., 2010). When the pH increased, the balance of Eqs. 2 and 3 moved to the right successively, accompanying NH^+_4 hydration reaction occurred and transformed into $NH_{3(aq)}$, and into $NH_{3(gas)}$. The Step II is accomplished by contacting the high concentration $NH_{3(gas)}$ with a gas (usually air) that does not initially contain ammonia (Bolado-Rodríguez et al., 2010), resulting in escape $NH_{3(gas)}$ from the water and was removed subsequently. Thus, the whole NH_4^+-N removal process mainly depends on pH and mass transfer rate.

3.3. Optimum removal processes

Optimum experimental conditions were first examined for NH_4^+-N removal by using simulated wastewater, in order to choose the best NH_4^+-N removal efficiency out of five different removal processes under different initial pH conditions after stripping for 150 min and the results are shown in Fig. 5. As can be seen from Fig. 5, in ceramsite process, pH changes had no effect on the removal rate of NH_4^+-N, the removal rates of NH_4^+-N were less than 10%. The removal mechanism of ceramsite process was proposed as a combination of ion exchange and molecule adsorption based on the influence of pH on their ammonium adsorption (Yang et al., 2015). Compared with ceramsite process, the removal rates of NH_4^+-N were enhanced in CCMH process at all the investigated pH values. This may be due to CCMH has higher S_{BET} and larger average pore volume than that of ceramsite (Fig. 4), being favorable for NH_4^+-N adsorption. In air stripping process, as expected, pH level gave bigger influence to the removal rate of NH_4^+-N. At acidic (pH=3) and neutral (pH=7) conditions, the removal rates of NH_4^+-N were only 6.7% and 24.2%, respectively.

The removal efficiency rapidly rose to 63.3% at alkaline (pH=11) condition. By raising pH levels, the removal mechanisms can be expressed by Eqs. 2 and 3. In ceramsite coupled with air stripping process, the initial pH has greater influence on the NH_4^+-N removal efficiency. The removal rates of NH_4^+-N were improved in the pH values of 7 and 11 compared to air stripping process, mainly contributed by the presence of ceramsite, as it enhanced the mass transfer in the

stripping system (Hartman et al., 2007), prompting Eq. 3 moved to the right, resulting in $NH_{3(gas)}$ diffuse into the air. In CCMH coupled with air stripping process, the removal rate of NH_4^+-N was more than 90% at all the investigated pH values, without being influenced by the initial pH. Several reasons may be adduced to the phenomenon that on the one hand, when the pH of the combined system was below 7, MH will be take place hydrolytic reaction (seen Eq. 4), and one of the resultant hydrolytic reaction product is hydroxyl ions (OH^-), resulting in increased the pH value, and promoting stripping efficiency. On the other hand, owing to CCMH has well-developed porous structure and high S_{BET}, its presence can improve the mass transfer of the stripping (Yuan et al., 2012), prompting Eq. 3 moved to the right, accelerating air stripping.

$$Mg(OH)_2 = Mg^{2+} + 2OH^- \quad (4)$$

Taken together, the highest removal efficiency for the NH_4^+-N concentration of 450 mg/L were obtained in the CCMH coupled with air stripping process under different pH conditions after stripping for 150 min. Therefore, the research was continued using the CCMH coupled with air stripping process to investigate the effect of other factors on the NH_4^+-N removal efficiency.

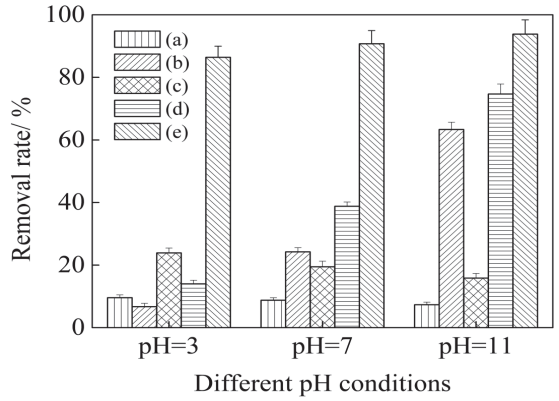

Fig. 5. The influence of (a) ceramsite, (b) air stripping, (c) CCMH, (d) ceramsite coupled with air stripping and (e) CCMH coupled with air stripping on the removal efficiency of NH_4^+-N from aqueous solution under different initial pH conditions after stripping for 150 min. Experimental condition: dosage of ceramsite was 3.5 g, dosage of CCMH was 3.5 g, initial concentration of NH_4^+-N was 450 mg/L and air flow rate was 0.8 L/min

3.4. Effect of initial pH

The wastewater containing NH_4^+-N, discharged from industries has a wide range of pH values. For air stripping process, many researchers have been reported that perfect removal efficiency was obtained when the pH above 7 (Guo et al., 2010). However, the effect of pH below 7 on the removal efficiency has been rarely investigated. In this study, the effect of initial pH on the removal of NH_4^+-N by CCMH coupled with air stripping process was depicted in Fig. 6(a), in which the variation of initial pH is determined with stripping time. From the Figure, it can be observed that as the pH increased in the range of 3-11, the removal efficiency of NH_4^+-N increased gradually and reached a maximum value after stripping for 150 min, when its initial pH 7 and 11, the removal rates were 90.8% and 93.8%, respectively. The same results also have been gotten by other researchers (Subramonian and Wu, 2014). Interestingly, when the initial pH was 3, the removal rate of NH_4^+-N by the combined process was still very high after stripping for 150 min, about 86.4%. It is clearly demonstrating that the initial pH, included acidic (pH=3), neutral (pH=7) and alkaline (pH=11) conditions, had only a negligible effect on the removal rate of NH_4^+-N by the combined process.

The reason is mainly because of the fact that in the presences of hydrogen ion (H^+), the MH is unstable and hydrolyzes easily in aqueous solution (Eq. 4), the major hydrolyzed product is hydroxyl radicals (-OH), which may be promote air stripping through neutralization reaction with H^+.

Table 2. Estimated general first-order rate constant (k) for NH_4^+-N removal at different experimental conditions

Experimental conditions		***k×10^{-2}/ min^{-1}***	***R^2***
pH	3	1.32	0.9777
	7	1.68	0.9808
	11	1.67	09952
Air flow rate (L/min)	0.4	1.07	0.9702
	0.8	1.68	0.9805
	1.6	2.09	0.9678

To compare NH_4^+-N removal rates, the obtained experimental data were fitted to a general first-order expression as shown in Eq. 5 (Park and Kim, 2015), and the values of the general first-order rate constant (k) were determined.

$$\frac{d[NH^+_4 - N]}{dt} = -k[NH^+_4 - N] \quad (5)$$

The removal kinetics of NH_4^+-N by the combined process at various initial pH are reflected in Fig. 6(b) and Table 2. It was indicated that plotting the natural logarithm of NH_4^+-N concentration versus stripping time yielded reasonably straight lines. In neutral (pH=7) and alkaline (pH=11) conditions, the kinetic data could be described well by the general first-order models, with high values of correlation coefficient (R^2) were 0.9808 and 0.9952, respectively, similar to the results obtained by previously experimental researches (Wu et al., 2015). In acidic (pH=3) condition, the kinetic data were also well described by the general first-order model, which correlation coefficient was 0.9777. The rate constant (k) for NH_4^+-N removal increased nearly 21% (from 1.32 to 1.67×10^{-2}/min) when the initial pH increased from 3 to 11.

3.5. Effect of air flow rate

The effect of air flow rates on the removal efficiency of NH_4^+-N by CCMH coupled with air stripping process were investigated at the speed of 0.4, 0.8 and 1.6 L/min and the results are depicted in Fig. 7(a), which illustrated that the removal rate increased as the air flow rate was increased. After stripping for 150 min, the removal rates were 80.2%, 90.8% and 95.9% for the air flow rates of 0.4, 0.8 and 1.6 L/min, respectively. The reason may be because higher feed velocity could promote the turbulence of feed solutions and decrease the mass transfer boundary layer thickness (Liu and Wang, 2016).

The removal kinetics of NH_4^+-N by the combined process at various air flow rates are listed in Fig. 7(b) and Table 2. From Fig. 7(b), it was found that plotting the natural logarithm of NH_4^+-N concentration versus stripping time yielded reasonably straight lines, with the correlation coefficients (R^2) were 0.9702, 0.9805 and 0.9678 at 0.4, 0.8 and 1.6 L/min, respectively, confirming that the removal of NH_4^+-N by the combined process at different ranges of air flow rates well followed the general first-order models. As detailed in Table 2, the rate constant (k) for the NH_4^+-N removal increased from 1.07×10^{-2}/min at 0.4 L/min to 2.09×10^{-2}/min at 1.6 L/min, about one fold.

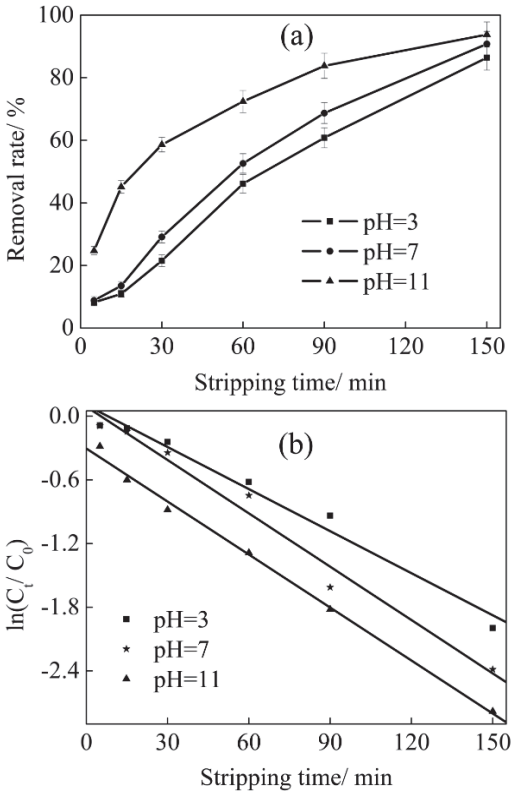

Fig. 6. (a) effect of initial pH on the removal of NH_4^+-N by CCMH coupled with air stripping and (b) the removal kinetics at various initial pH. Experimental condition: dosage of CCMH was 3.5 g, initial concentration of NH_4^+-N was 450 mg/L and air flow rate was 0.8 L/min

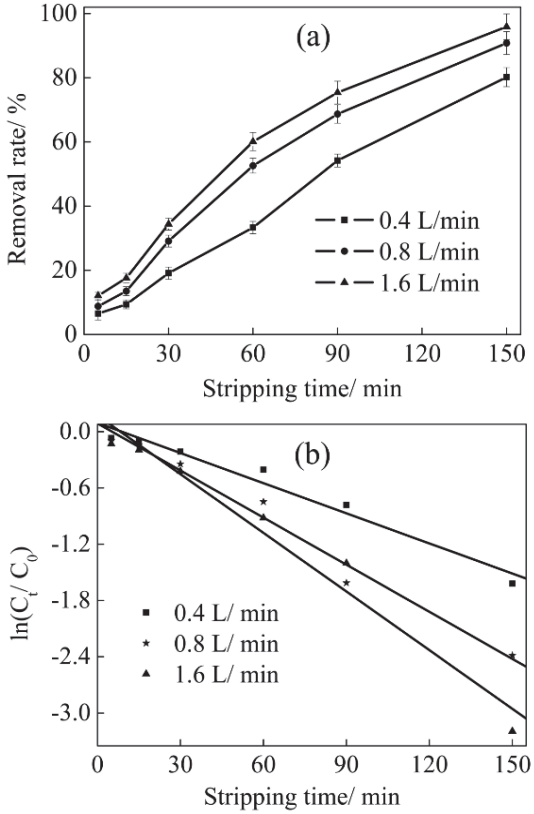

Fig. 7. (a) effect of air flow rate on the removal of NH_4^+-N by CCMH coupled with air stripping and (b) the removal kinetics at different air flow rates. Experimental condition: dosage of CCMH was 3.5 g, initial concentration of NH_4^+-N was 450 mg/L and initial pH was 6-7

4. Conclusions

The CCMH coupled with air stripping process has a good effect on the removal of NH_4^+-N from aqueous solution, without being influenced by the initial pH. The removal of NH_4^+-N by the combined process in all fractions (included initial pH and air flow rate), could be fitted by the general first-order model, with high correlation coefficients (R^2> 0.95).

Overall, the combined process could be used as a possible option for the removal of NH_4^+-N from aqueous solution, with no pH value adjustment required and is the more environmental friendly compared to the traditional air stripping technique.

Acknowledgments

This work was supported by the Fundamental Research Funds for the Central Universities of China (Project No. 15D111321), "Textile Light" Application Basic Research of China (Project No. J201503), Natural Science Foundation Training Project of Shandong Province, China (Project No. ZR2018PEE026) and Science and Technology Planning Project of Zaozhuang City, Shandong Province, China (Project No. 2018GX12).

References

Arslan A., Veli S., (2012), Zeolite 13X for adsorption of ammonium ions from aqueous solutions and hen

slaughterhouse wastewaters, *Journal of the Taiwan Institute of Chemical Engineers*, **43**, 393-398.

Ata O.N., Kanca A., Demir Z., (2017), Optimization of ammonia removal from aqueous solution by microwave-assisted air stripping, *Water Air and Soil Pollution*, **228**, 448-458.

Basahel S.N., Ali T.T., Mokhtar M., Narasimharao K., (2015), Influence of crystal structure of nanosized ZrO_2 on photocatalytic degradation of methyl orange, *Nanoscale Research Letters*, **10**, 73-86.

Bolado-Rodríguez S., García-Sinovas D., Álvarez-Benedí J., (2010), Application of pig slurry to soils. Effect of air stripping treatment on nitrogen and TOC leaching, *Journal of Environmental Management*, **91**, 2594-2598.

Ding J., Zhong Q., Gu H., (2018), Iron-titanium dioxide composite nanoparticles prepared with an energy effective method for efficient visible-light-driven photocatalytic nitrogen reduction to ammonia, *Journal of Alloys and Compounds*, **746**, 147-152.

Feng Z.M., Sun T., (2015), A novel selective hybrid cation exchanger for low-concentration ammonia nitrogen removal from natural water and secondary wastewater, *Chemical Engineering Journal*, **281**, 295-302.

Furlani E., Tonello G., Maschio S., Aneggi E., Minichelli D., Bruckner S., (2011), Sintering and characterisation of ceramics containing paper sludge, glass cullet and different types of clayey materials, *Ceramics International*, **37**, 1293-1299.

Guo J.S., Abbas A.A., Chen Y.P., Liu Z.P., Fang F., Chen P., (2010), Treatment of landfill leachate using a combined stripping, Fenton, SBR, and coagulation process, *Journal of Hazardous Materials*, **178**, 699-705.

Gustin S., Marinsek-Logar R., (2011), Effect of pH, temperature and air flow rate on the continuous ammonia stripping of the anaerobic digestion effluent, *Process Safety and Environmental Protection*, **89**, 61-66.

Hartman M., Trnka O., Pohorely M., (2007), Minimum and terminal velocities in fluidization of particulate ceramsite at ambient and elevated temperature, *Industrial and Engineering Chemistry Research*, **46**, 7260-7266.

Han W., Yue Q.Y., Wu S.P., Zhao Y.Q., Gao B.Y., Li Q., Wang Y., (2013), Application and advantages of novel clay ceramic particles (CCPs) in an up-flow anaerobic bio-filter (UAF) for wastewater treatment, *Bioresource Technology*, **137**, 171-178.

He H.T., Zhao P., Yue Q.Y., Gao B.Y., Yue D.D., Li Q., (2015), A novel polynary fatty acid/sludge ceramsite composite phase change materials and its applications in building energy conservation, *Renewable Energy*, **76**, 45-52.

Jr J.B., Oliviero L., Renard B., Duprez D., (2002), Catalytic wet air oxidation of ammonia over M/CeO_2 catalysts in the treatment of nitrogen-containing pollutants, *Catalysis Today*, **75**, 29-34.

Ji G.D., Zhou Y., Tong J.J., (2010), Nitrogen and phosphorus adsorption behavior of ceramsite material made from coal ash and metallic iron, *Environmental Engineering Science*, **27**, 871-878.

Kaza L., Sobhi H.F., Fruscella J.A., Kaul C., Thakur S., Perera N.I., Alexander K., Riga A.T., (2012), Thermal analysis of water and magnesium hydroxide content in commercial pharmaceutical suspensions milk of magnesia, *Journal of Thermal Analysis and Calorimetry*, **109**, 1365-1371.

Lee D.K., (2003), Mechanism and kinetics of the catalytic oxidation of aqueous ammonia to molecular nitrogen, *Environmental Science and Technology*, **37**, 5745-5749.

Li M., Kao H.T., Wu Z.S., Tan J.M., (2011), Study on preparation and thermal property of binary fatty acid and the binary fatty acids/diatomite composite phase change materials, *Applied Energy*, **88**, 1606-1612.

Li T.P., Sun T.T., Aftab T.B., Li D.X., (2017), Photocatalytic degradation of methylene blue in aqueous solution using ceramsite coated with micro-Cu_2O under visible-light irradiation, *Korean Journal of Chemical Engineering*, **34**, 1199-1207.

Li T.P., Sun T.T., Li D.X. (2018), Preparation, sintering behavior and expansion performance of ceramsite filter media from dewatered sewage sludge, coal fly ash and river sediment, *Journal of Material Cycles and Waste Management*, **20**, 71-79.

Limoli A., Langone M., Andreottola G., (2016), Ammonia removal from raw manure digestate by means of a turbulent mixing stripping process, *Journal of Environmental Management*, **176**, 1-10.

Liu H.Y., Wang J.L., (2016), Separation of ammonia from radioactive wastewater by hydrophobic membrane contactor, *Progress in Nuclear Energy*, **86**, 97-102.

Malovanyy A., Sakalova H., Yatchyshyn Y., Plaza E., Malovanyy M., (2013), Concentration of ammonium from municipal wastewater using ion exchange process, *Desalination*, **329**, 93-102.

Matsukevich I.V., Ruchets A.N., Krutko N.P., Vashuk V.V., Kuznetsova T.F., (2017), Effect of deposition conditions on properties of nanostructured magnesium hydroxide powders, *Russian Journal of Applied Chemistry*, **90**, 3-9.

Mittelman A.M., Lantagne D.S., Rayner J., Pennell K.D., (2015), Silver dissolution and release from ceramic water filters, *Environmental Science and Technology*, **49**, 8515-8522.

Park S., Kim M., (2015), Innovative ammonia stripping with an electrolyzed water system as pretreatment of thermally hydrolyzed wasted sludge for anaerobic digestion, *Water Research*, **68**, 580-588.

Pressley T.A., Bishop D.F., Roan S.G., (1972), Ammonia-nitrogen removal by breakpoint chlorination, *Environmental Science and Technology*, **6**, 622-628.

Reli M., Ambrozová N., Sihor M., Matejová L., Capek L., Obalová L., Matej Z., Kotarba A., Kocí K., (2015), Novel cerium doped titania catalysts for photocatalytic decomposition of ammonia, *Applied Catalysis B: Environmental*, **178**, 108-116.

Rubia M.Á.D.L., Walker M., Heaven S., Banks C.J., Borja R., (2010), Preliminary trials of in situ ammonia stripping from source segregated domestic food waste digestate using biogas: Effect of temperature and flow rate, *Bioresource Technology*, **101**, 9486-9492.

Song W.L., Li Z.P., Liu F., Ding Y., Qi P.S., You H., Jin C., (2018), Effective removal of ammonia nitrogen from waste seawater using crystal seed enhanced struvite precipitation technology with response surface methodology for process optimization, *Environmental Science and Pollution Research*, **25**, 628-638.

Subramonian W., Wu T.Y., (2014), Effect of enhancers and inhibitors on photocatalytic sunlight treatment of methylene blue, *Water Air and Soil Pollution*, **225**, 1922-1937.

Tai C.Y., Tai C.T., Chang M.H., Liu H.S., (2007), Synthesis of magnesium hydroxide and oxide nanoparticles using a spinning disk reactor, *Industrial and Engineering Chemistry Research*, **46**, 5536-5541.

Wang C., Zhang F.S., (2013), Zeolite loaded ceramsite developed from construction and demolition waste, *Materials Letters*, **93**, 380-382.

Wang J.H., Zhou W.G., Yang H.Z., Wang F., Ruan R., (2015), Trophic mode conversion and nitrogen deprivation of microalgae for high ammonium removal from synthetic wastewater, *Bioresource Technology*, **196**, 668-676.

Wang Z., Zhong M.G., Wan J.F., Xu G.J., Liu Y., (2016), Development of attapulgite composite ceramsite/quartz sand double-layer biofilter for micropolluted drinking source water purification, *International Journal of Environmental Science and Technology*, **13**, 825-834.

Wu L., Chen S.P., Zhou J.S., Zhang C., Liu J.Y., Luo J.H., Song G.Y., Qian G.R., Song L.J., Xia M., (2015), Simultaneous removal of organic matter and nitrate from bio-treated leachate via iron-carbon internal micro-electrolysis, *RSC Advances*, **5**, 68356-68360.

Xu G.R., Zou J.L., Li G.B., (2009), Stabilization/solidification of heavy metals in sludge ceramsite and leachability affected by oxide substances, *Environmental Science and Technology*, **43**, 5902-5907.

Yetilmezsoy K., Sapci-Zengin Z., (2009), Recovery of ammonium nitrogen from the effluent of UASB treating poultry manure wastewater by MAP precipitation as a slow release fertilizer, *Journal of Hazardous Materials*, **166**, 260-269.

Yang L., Wei J., Liu Z.Y., Wang J.L., Wang D.T., (2015), Material prepared from drinking waterworks sludge as adsorbent for ammonium removal from wastewater, *Applied Surface Science*, **330**, 228-236.

Yuan M.H., Chen Y.H., Tsai J.Y., Chang C.Y., (2016), Removal of ammonia from wastewater by air stripping process in laboratory and pilot scales using a rotating packed bed at ambient temperature, *Journal of the Taiwan Institute of Chemical Engineers*, **60**, 488-495.

Yuan S.Z., Lu H., Wang J., Zhou J.T., Wang Y., Liu G.F., (2012), Enhanced bio-decolorization of azo dyes by quinone-functionalized ceramsites under saline conditions, *Process Biochemistry*, **47**, 312-318.

Zhang L.N., Xu B.H., Gong J.D., Bu T.D., (2010), Membrane combination technic on treatment and reuse of high ammonia and salts wastewater in rare earth manufacture process, *Journal of Rare Earths*, **28**, 501-503.

Zhang X.N., Mao G.Y., Jiao Y.B., Shang Y., Han R.P., (2014), Adsorption of anionic dye on magnesium hydroxide-coated pyrolytic bio-char and reuse by microwave irradiation, *International Journal of Environmental Science and Technology*, **11**, 1439-1448.

Zhou X.Q., Zhao J.Y., Li Z.F., Song J.N., Li X.Y., Yang X., Wang D.L., (2016), Enhancement effects of ultrasound on secondary wastewater effluent disinfection by sodium hypochlorite and disinfection by-products analysis, *Ultrasonics Sonochemistry*, **29**, 60-66.

Zou W.H., Liu L., Li H.P., Han X.L., (2016), Investigation of synergistic adsorption between methyl orange and Cd(II) from binary mixtures on magnesium hydroxide modified clinoptilolite, *Korean Journal of Chemical Engineering*, **16**, 1-11.